International Conference on Mathematics, Computational Methods & Reactor Physics (M&C 2009)
Saratoga Springs, New York, May 3-7, 2009, on CD-ROM, American Nuclear Society, LaGrange Park, IL (2009)

RADIATIVE TRANSFER WITH MONTE CARLO PREDICTOR-CORRECTOR METHODS

Jesse Cheatham, James Paul Holloway, and William R. Martin
Department of Nuclear Engineering and Radiological Sciences
University of Michigan, Ann Arbor, Michigan 48109, USA
cjesse@umich.edu; hagar@umich.edu; wrm@umich.edu;

ABSTRACT

In this paper we explore the time discretation error introduced into the Implicit Monte Carlo (IMC) method and contrast IMC with the Carter-Forest (CF) method which should be more accurate. The IMC method is the current standard even though it makes two approximations to solve the linear Radiative Transfer (RT) equations while the CF method solves them exactly. When the opacity and β are functions of temperature, both IMC and CF must approximate the values of the opacity and β as constant during a time step, adding a source of error to both methods. To determine the effect of the approximations in the IMC and CF methods, a detailed analysis was conducted to quantify the accumulated effect of each assumption. The residual analysis demonstrates the existence of a bias in the IMC method based on the value of alpha, and the truncation analysis shows that a significant source of truncation error in both the IMC and CF method originates with the constant opacity approximation over a time step in a non-linear problem. A predictor-corrector method is demonstrated that changes the CF method to be second order accurate in 0D while the IMC method will remain first order accurate.

Key Words: IMC, CF, Truncation Error

1. INTRODUCTION

The current standard for Monte Carlo Radiative Transfer (MCRT) methods is the Implicit Monte Carlo (IMC) Method [1] proposed by Fleck and Cummings. IMC simplifies the nonlinear radiative transfer equations by making four separate approximations (two native to IMC) which together produce an $O(\Delta t)$ error in the solution. Despite these approximations, the IMC method is fairly robust and reliably converges to equilibrium solutions. In 1973 Carter and Forest [2] proposed a different method for MCRT that makes only two of the approximations used in IMC, and therefore had the potential to be more accurate. In this paper the error introduced into both the IMC and Carter-Forest (CF) methods is explored and a more accurate predictor-corrector method is proposed.

The 0-D gray radiative transfer equations are

$$\frac{1}{c}\frac{d\phi(t)}{dt} + \sigma(t)\phi(t) = c\sigma(t)U_r(t) \tag{1}$$

$$\frac{dU_m(t)}{dt} + c\sigma(t)U_r(t) = \sigma(t)\phi(t) \tag{2}$$

$$\frac{1}{\beta(t)}\frac{dU_r(t)}{dt} + c\sigma(t)U_r(t) = \sigma(t)\phi(t) \tag{3}$$

where $\phi(t)$ is the photon flux, $U_m(t)$ is the material energy density, and $\sigma(t)$ is the interaction cross section or opacity. Equations (2) and (3) are physically equivalent formulations of the material energy balance equation and $\beta(t)$ relates U_m to U_r through

$$\beta(t) = \frac{dU_r(t)}{dU_m(t)}. \tag{4}$$

The material energy density $U_m(t)$ is related to the material temperature T by integration of the specific heat, $U_m(t) = \int_0^T C_v(T)dT$. The equilibrium radiation density, $U_r(t)$, is related to the material temperature by $U_r(t) = aT^4$ where $a = 8k^4\pi/(15c^3h^3)$ is the radiation constant, c is the speed of light, k is Boltzmann's constant and h is Planck's constant.

Equation (1) is the photon transport equation while Eqs. (2) and (3) represent two mathematically equivalent forms of the material energy balance equations. Equation (2) is used for the conservation of energy and material energy update, and Eq. (3) is used in the computational solution of the transport equation. To solve (1) and (3) both IMC and CF approximate $\sigma(t)$ and $\beta(t)$ as constant during a time step, typically as

$$\beta(t) \approx \beta(t_n) + O(\Delta t) \tag{5}$$
$$\sigma(t) \approx \sigma(t_n) + O(\Delta t)\,. \tag{6}$$

Equations (5) and (6) are the only approximations made in the nonlinear 0-D CF method.

2. Residual Error Analysis of the 0D Grey RT Linear Problem

Analytic solutions have been produced for the 0D Grey Radiative Transfer equations with constant opacity and a heat capacity $C_v(T) = C_vT^3$. While not physically meaningful, this problem formulation linearizes the Grey RT equations and gives insight into the methods used to solve them..

The analytic solution [3] to the Carter-Forest formulation of the gray RT problems yields

$$\phi(t_{n+1}) = \phi(t_n) + \frac{c^2\sigma\beta Q_o\Delta t}{\gamma} + \left[\frac{c^2\sigma}{\gamma}U_r(t_n) - \frac{c\sigma}{\gamma}\phi(t_n)\right](1-e^{-\gamma\Delta t}) - \left[\frac{cQ_o}{\gamma} - \frac{c^2\sigma\beta Q_o}{\gamma^2}\right](1-e^{-\gamma\Delta t}) \tag{7}$$

where $\gamma = c\sigma(1+\beta)$. It is worth noting that in this particular problem, the solution to the CF method is exact within a time step while the Implicit Monte Carlo (IMC) analytic solution [4],

$$\phi(t_{n+1}) = \phi(t_n)e^{-c\sigma f(\Delta t)} + [cU_r(t_n) + \frac{Q_o}{\sigma f}]\left(1 - e^{-c\sigma f(\Delta t)}\right) \tag{8}$$

is not exact within a time step. The residual error of the IMC is determined to by subtracting the IMC estimation of $\phi(t_{n+1})$ from the CF value of $\phi(t_{n+1})$ to quantify the error in the IMC approximations.

$$\phi_{CF}(t_{n+1}) - \phi_{IMC}(t_{n+1}) = \phi(t_n) + \frac{c^2\sigma\beta Q_o\Delta t}{\gamma} + \frac{c^2\sigma}{\gamma}U_r(t_n) - \frac{c\sigma}{\gamma}\phi(t_n) + \frac{cQ_o}{\gamma} - \frac{c^2\sigma\beta Q_o}{\gamma^2} \tag{9}$$
$$- \frac{c^2\sigma}{\gamma}U_r(t_n)e^{-\gamma\Delta t} + \frac{c\sigma}{\gamma}\phi(t_n)e^{-\gamma\Delta t} - \frac{cQ_o}{\gamma}e^{-\gamma\Delta t} + \frac{c^2\sigma\beta Q_o}{\gamma^2}e^{-\gamma\Delta t}$$
$$- \phi(t_n)e^{-c\sigma f\Delta t} - cU_r(t_n) + cU_r(t_n)e^{-c\sigma f\Delta t} - \frac{Q_o}{\sigma f} + \frac{Q_o}{\sigma f}e^{-c\sigma f\Delta t}.$$

Similar terms are grouped from Equation (9) as follows

$$R_\phi = \phi(t_n) - \frac{c\sigma}{\gamma}\phi(t_n) + \frac{c\sigma}{\gamma}\phi(t_n)e^{-\gamma\Delta t} - \phi(t_n)e^{-c\sigma f\Delta t}. \tag{10}$$

Expanding around $\Delta t = 0$, the exponentials may be rewritten as

$$e^{-\gamma\Delta t} \approx 1 - \gamma\Delta t + \frac{\gamma^2\Delta t^2}{2} + O(\Delta t^3) \tag{11}$$

and

$$e^{-c\sigma f\Delta t} \approx 1 - c\sigma f\Delta t + \frac{c^2\sigma^2 f^2\Delta t^2}{2} + O(\Delta t^3) \tag{12}$$

Substituting Equations (12) and (11) into (10) yields

$$R_\phi = c\sigma\phi(t_n)\Delta t\left[(f-1) + \frac{\gamma\Delta t}{2} - \frac{c\sigma f^2\Delta t}{2}\right] + O(\Delta t^3). \tag{13}$$

Now, Taylor expand the Fleck factor with the assumption that $\alpha\beta c\sigma\Delta t \approx 0$ as

$$f = \frac{1}{1+\alpha\beta c\sigma\Delta t} \approx 1 - \alpha\beta c\sigma\Delta t + \frac{\alpha^2\beta^2c^2\Delta t^2}{2} + O(\Delta t^3). \tag{14}$$

Using the Fleck factor expansion and neglecting terms that are $O(\Delta t^2)$ the residual for $\phi(t_n)$ terms becomes

$$R_\phi = c\sigma\phi(t_n)\Delta t\left[-\alpha\beta c\sigma\Delta t + \frac{\beta c\sigma\Delta t}{2}\right] + O(\Delta t^3). \tag{15}$$

Next, the source terms are grouped together as

$$R_{Q_o} = \frac{\beta c^2\sigma Q_o\Delta t}{\gamma} + \frac{cQ_o}{\gamma} - \frac{\beta c^2\sigma Q_o}{\gamma^2} - \frac{cQ_o}{\gamma}e^{-\gamma\Delta t} + \frac{\beta c^2\sigma Q_o}{\gamma^2}e^{-\gamma\Delta t} - \frac{Q_o}{\sigma f} + \frac{Q_o}{\sigma f}e^{-c\sigma f\Delta t}. \tag{16}$$

Expanding the exponentials by using Equations (11) and (12) yields

$$R_{Q_o} = \frac{\beta c^2\sigma Q_o\Delta t^2}{2} - \frac{cQ_o\gamma\Delta t^2}{2} + \frac{c^2\sigma f Q_o\Delta t^2}{2} + O(\Delta t^3), \tag{17}$$

which is simplified again by expanding the Fleck factor f to give the expected small truncation error result

$$R_{Q_o} = O(\Delta t^3). \tag{18}$$

Finally, the $U_r(t_n)$ terms are grouped together as

$$R_{U_r} = \frac{c^2\sigma}{\gamma}U_r(t_n) - \frac{c^2\sigma}{\gamma}U_r(t_n)e^{-\gamma\Delta t} - cU_r(t_n) + cU_r(t_n)e^{-c\sigma f\Delta t}. \quad (19)$$

Simplify by expanding the exponentials in Equation (19) to get

$$R_{U_r} = c^2\sigma U_r(t_n)\Delta t - \frac{c^2\sigma\gamma\Delta t^2}{2}U_r(t_n) - c^2\sigma f\Delta t U_r(t_n) + \frac{c^3\sigma^2 f^2\Delta t^2}{2}U_r(t_n) + O(\Delta t^3), \quad (20)$$

and expanding the Fleck factor f will yield the final U_r residual,

$$R_{U_r} = \alpha\beta c^3\sigma^2\Delta t^2 U_r(t_n) - \frac{\beta c^3\sigma^2\Delta t^2}{2}U_r(t_n) + O(\Delta t^3). \quad (21)$$

Combining the residual terms from Equations (15), (18), and (21) yields the residual error of the IMC equations

$$R = \alpha\beta c^3\sigma^2\Delta t^2 U_r(t_n) - \frac{\beta c^3\sigma^2\Delta t^2}{2}U_r(t_n) + \frac{\beta c^2\sigma^2\Delta t^2\phi(t_n)}{2} - \alpha\beta c^2\sigma^2\Delta t^2\phi(t_n) + O(\Delta t^3)$$

It is worth noting that the IMC method will be $O(\Delta t)$ globally unless $\alpha = 0.5$ in which case the IMC method will be $O(\Delta t^2)$ globally. In practice α is always set to be equal to 1 to address stability concerns.

In the case of $\alpha = 1$ the residual term may be simplified to

$$R = c^2\beta\sigma^2\Delta t^2\left[c\frac{U_r}{2} - \frac{\phi(t_n)}{2}\right]. \quad (22)$$

It is important to consider the types of problems being solved when examining the residual error. In particular, for warming problems $\phi(t_n) \gg U_r(t_n)$ meaning that the residual will be negative. In other words, the IMC method will store more energy into the photon field $\phi(t)$ than it should, leaving a cooler material temperature T. Of course this is only of concern during a transient since at equilibrium $\phi(t_n) \approx U_r(t_n)$.

3. IMC and CF Derivation

Besides the approximations to $\beta(t)$ and $\sigma(t)$, the IMC method also makes the assumption that

$$U_r(t) \approx \alpha U_r(t_{n+1}) + (1-\alpha)U_r(t_n) + O(\Delta t) \quad (23)$$

where α is a user defined parameter usually set equal to unity. Inserting (23) into (3), integrating over a time step and solving for $U_r(t_{n+1})$ yields

$$U_r(t_{n+1}) = \frac{U_r(t_n) + (\alpha-1)\beta_n c\sigma_n\Delta t U_r(t_n)}{1+\alpha\beta_n c\sigma_n\Delta t} + \frac{\beta_n\sigma_n\int_{t_n}^{t_{n+1}}\phi(t')dt'}{1+\alpha\beta_n c\sigma_n\Delta t} + O(\Delta t^2). \quad (24)$$

The second IMC specific approximation is $\int_{t_n}^{t_{n+1}}\phi(t')dt' \approx \Delta t\phi(t) + O(\Delta t^2)$, which physically means that all photon re-emissions occur instantly after absorption. Substituting the resulting expression for $U_r(t_{n+1})$ into (23) yields the IMC approximation to $U_r(t)$

$$U_r(t) = fU_r(t_n) + \frac{1-f}{c}\phi(t) + O(\Delta t) \quad (25)$$

where the Fleck factor f is defined as

$$f = \frac{1}{1 + \alpha\beta_n c\sigma_n \Delta t}\,. \tag{26}$$

Now (25) is substituted into (1) giving the IMC transport equation

$$\frac{1}{c}\frac{d\phi(t)}{dt} + f\sigma_n\phi(t) = c\sigma_n f U_r(t_n) + O(\Delta t)\,. \tag{27}$$

The IMC approximation and linearization of $\sigma(t)$ and $\beta(t)$ create multiple sources of $O(\Delta t)$ error to (27). Integrating over a time step yields the deterministic 0-D IMC approximation with explicit truncation error,

$$\phi(t_{n+1}) = \phi(t_n)e^{-c\sigma_n f\Delta t} + cU_r(t_n)(1 - e^{-c\sigma_n f\Delta t}) + O(\Delta t^2) \tag{28}$$

The error in (28) is locally $O(\Delta t^2)$ and $O(\Delta t)$ globally in the numerical scheme [5].

The Carter-Forest method makes only the approximations shown in (5) and (6) and then solves Eqs. (1) and (3), yielding

$$U_r(t) = U_r(t_n)e^{\int_{t_n}^{t} -c\beta(t'')\sigma(t'')dt''} + \int_{t_n}^{t} \phi(t')\beta(t')\sigma(t')e^{\int_{t'}^{t} -c\beta(t'')\sigma(t'')dt''}dt'\,. \tag{29}$$

Substituting Eq. (29) into (1) and integrating over a time step with $\sigma(t)$ and $\beta(t)$ constant yields

$$\begin{aligned}\phi(t_{n+1}) = \phi(t_n) - \int_{t_n}^{t_{n+1}} c\sigma_n\phi(t)dt + \int_{t_n}^{t_{n+1}} c^2\sigma_n U_r(t_n)e^{-c\beta_n\sigma_n(t-t_n)}dt \\ + \int_{t_n}^{t_{n+1}} \sigma_n \int_{t_n}^{t} \beta_n\sigma_n\phi(t')e^{-c\beta_n\sigma_n(t-t')}dt'dt + O(\Delta t^2).\end{aligned} \tag{30}$$

Like the IMC method (30) yields an $O(\Delta t^2)$ local error, so the CF approach will also yield a global error of $O(\Delta t)$. So even though the Carter-Forest method makes fewer approximations, it still suffers from the same order of error. However, unlike IMC, the approximation of $\sigma(t)$ is the main source of error. Therefore, a higher order approximation of $\sigma(t)$ should yield a higher order error in the numerical calculation. Although this paper does make use of the fact that $\beta(t) \cdot \sigma(t) =$ Constant, the truncation analysis shows that the $\beta(t)$ approximation yields a higher order error than the IMC approximation and the $\sigma(t)$ approximation, and therefore can be neglected. These analytic results have been confirmed in 0D numerical modeling.

A better approximation of $\sigma(t)$ can be achieved by

$$\sigma(t_{n+\frac{1}{2}}) = \frac{\sigma(t_{n+1}) + \sigma(t_n)}{2} + O(\Delta t^2) \tag{31}$$

where the value $\sigma(t_{n+1})$ is approximated by using a Monte Carlo predictor step which is $O(\Delta t^2)$ accurate since it is a local-in-time estimate. Once the value of $\sigma(t_{n+1})$ is calculated, the Monte Carlo method is applied again but now with the opacity $\sigma(t_{n+\frac{1}{2}})$ instead of $\sigma(t_n)$. When the predictor-corrector opacity estimation is applied to the IMC method, there is no change in the $O(\Delta t)$ global error (for $\alpha \neq 0.5$). However, the Carter-Forest method changes to a globally $O(\Delta t^2)$ method since the approximation to $\sigma(t)$ is the only global $O(\Delta t)$ source of error.

The down side of applying a predictor-corrector method is that the computational time for a single time step is effectively doubled. To minimize the additional work a predictor-corrector creates, a variable weight predictor-corrector is implemented. A variable weight predictor step uses significantly fewer predictor particles at a higher "weight" to simulate larger packets of photons; the corrector step then uses the originally designated number of photon packages to complete the time step. Due to Monte Carlo noise, the variable weight predictor using fewer particles yields a less precise estimate of $\sigma(t_{n+1})$ but the estimate may be satisfactory.

While a simple time average of σ has been proposed above, other approaches could be used. The temperature estimate proposed by A. Wollaber and E. Larsen [6] assumes a functional form of the opacity $\sigma(t) = \gamma/T(t)^3$, and that temperature change is approximately linear over a small time step. Then the average value of $\sigma(t)$ is preserved by

$$\bar{\sigma} = \frac{1}{\Delta t}\int_{t_n}^{t_{n+1}} \frac{\gamma}{T(t)^3} dt = \frac{\gamma}{T_*^3} \tag{32}$$

where

$$T_* = \left[\frac{T_n^2 T_{n+1}^2}{(T_{n+1}+T_n)/2}\right]^{1/3}. \tag{33}$$

Note that $T_* \approx \frac{T_n+T_{n+1}}{2}$ for small time steps. The 1D predictor-corrector implementation does not update the number of particles that a material should emit during a corrector step due to the higher temperature during that time step and the knowledge that $\beta(t)\cdot\sigma(t) =$ Constant is used.

4. 0D Numerical Results

A 0-D test problem was studied in which the material is set to a starting temperature of $T = 0.1$, $\sigma(t)$ varies as $1000/T^3$, and $\beta(t) = 40 \cdot T^3$. An instantaneous source occurs at the start of the problem with $Q(t) = 1000cU_r(t)\delta(t)$ with $\alpha = c = 1$.

Figure 1 shows the relative error from a benchmark solution created with Carter-Forest, and problem runs using CF and IMC methods. The relative error of the material temperature is plotted vs. time-step size for the given times $t = 1\times10^{-5}$, 5×10^{-5}, and 1×10^{-4}. Both methods are $O(\Delta t)$ accurate. It is worth noting that the IMC method appears more accurate at a later time in the problem, which appears to conflict directly with the anticipation that the CF method is more accurate. It should be noted that in this warming problem, when the opacity $\sigma(t)$ is held constant during a time step, the opacity remains too large for too long, resulting in the absorption of more energy then physically correct. As shown in equation (22), when $\alpha = 1$ the material temperature will be lower than what is supposed to be modeled, offsetting the large unphysical temperature gain due to incorrect opacity estimation.

Figure 2 is arranged the same as Figure 1, except predictor-corrector methods were used instead of the standard methods. While the IMC method still yields $O(\Delta t)$ error, the CF method now shows $O(\Delta t^2)$ global error. This result is anticipated by the truncation analysis since the CF method was dominated by the approximation of $\sigma(t)$ while the IMC method was dominated by both the approximation of $\sigma(t)$ and the assumption of the functional form the of equilibrium radiation density $U_r(t)$.

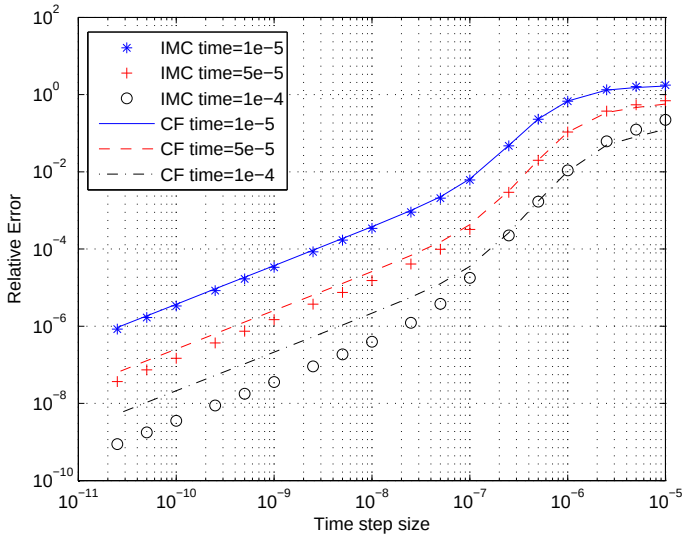

Figure 1. Relative error in material temperature vs. time step size for the 0-D problem.

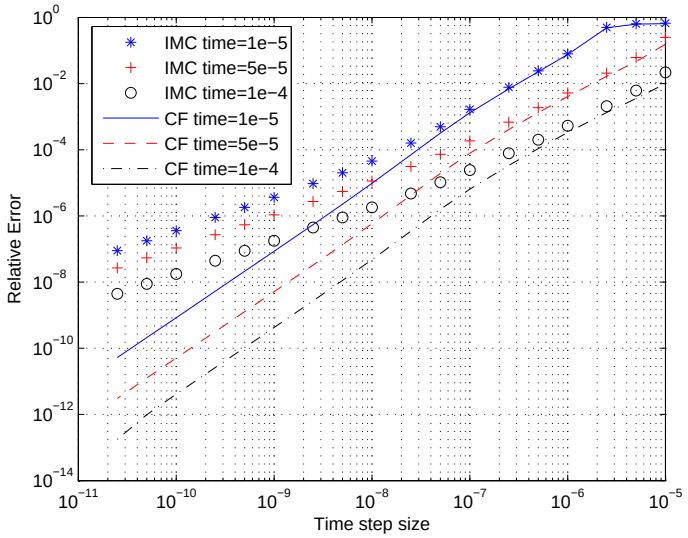

Figure 2. Relative error in material temperature vs. time step size for the 0-D problem using predictor-corrector methods.

5. 1D Numerical Results

Next, a 1-D problem is examined to determine the effect of predictor-corrector methods on a Marshak wave problem. A significant difference between the 0-D and 1-D methods is the spatial dependence of material emission after an absorption. In a 1-D code, a photon that is absorbed in a spatial region raises the temperature of the entire region. When an emission occurs from the material region during the next time step, a photon may be emitted from anywhere within the spatial region, not simply from where the particle was absorbed. Effectively this re-emission process is tantamount to photons traveling faster than the speed of light. To minimize the unphysical transport of photons, the emission from a material spatial region is biased by examining the emission due to temperature from the regions directly adjacent to it [7] . A typical Marshak wave will progress from one side of the region in question to the other side, and therefore the weighting scheme will "slow" the Marshak wave to a more realistic speed since photon emission will be biased towards the side of the cell where the Marshak wave entered.

A parameter study was conducted on a 1-D problem with vacuum boundary conditions, a 1 keV isotropic source on the $x = 0$ boundary, $C_v = 1/0.14$, $a = c = 1$, $\Delta t = \Delta\tau C_v$, and the starting temperature of $T_0 = 0.1$. The heat capacity C_v is constant and $\sigma(t) = 1/T^3(t)$ and $\beta(t) = \big(4a/C_v\big)T^3(t)$. By varying the values of $\Delta\tau$ and the width Δx, the differences between the standard approach to IMC and CF are examined with and without predictor-corrector methods. The L_1 error for the material temperature is computed based on a benchmark temperature solution. Eighty million source particles were used to simulate this 1-D Monte Carlo problem. Tables I-VI show the different methods at different time steps and cell widths at the value $\tau = 20$ to show the effectiveness of the methods.

Table I. IMC L1 Norm From Reference Solution for Each Spatial Width

$\Delta\tau\backslash\Delta x$	0.025	0.05	0.1
0.01	0.00161	0.00196	0.00171
0.02	0.00327	0.00375	0.00360
0.04	0.00623	0.00721	0.00679
0.05	0.00730	0.00852	0.00841
0.08	0.01162	0.01269	0.01265
0.1	0.01507	0.01495	0.01527

Tables I and IV indicate that the CF method yields a more accurate solution than the IMC method for each input parameter at the given time $\tau = 20$. Both CF and IMC predictor-corrector methods give an improved estimate of the entire Marshak wave at a given time τ shown in Tables II and V at the cost of increased computation time. Predictor-Corrector methods have the largest effect at the front of the Marshak wave, shown in Figure 3, which is not surprising since that is where the approximation to $\sigma(t)$ is the most inaccurate over a time step.

Table II. IMC with Predictor-Corrector L1 Norm From Reference Solution for Each Spatial Width

$\Delta\tau\backslash\Delta x$	0.025	0.05	0.1
0.01	0.00097	0.00169	0.00169
0.02	0.00226	0.00328	0.00299
0.04	0.00481	0.00568	0.00587
0.05	0.00583	0.00693	0.00729
0.08	0.00892	0.01047	0.01122
0.1	0.01093	0.01257	0.01353

Table III. IMC with 100 Variable Weight Predictor-Corrector L1 Norm From Reference Solution for Each Spatial Width

$\Delta\tau\backslash\Delta x$	0.025	0.05	0.1
0.01	0.00152	0.00183	0.00152
0.02	0.00228	0.00299	0.00319
0.04	0.00471	0.00584	0.00603
0.05	0.00595	0.00710	0.00746
0.08	0.00897	0.01050	0.01117
0.1	0.01099	0.01255	0.01353

To reduce computational effort of predictor-corrector methods, variable weight predictor-corrector (VWPC) methods are used with $1/100$ the number of particles for the predictor step and the normal number of particles for the corrector step. We call this method 100 variable weight predictor-corrector though clearly other multiples for the number of predictor particles can be used. The error for the VWPC methods is shown in Tables III and VI. Like traditional predictor-correctors, they can improve the accuracy of the solution but require less computational effort.

The importance of the computational cost in these methods is hard to quantify for a research code. For completeness, Figures 4 and 5 plot the relative error vs. the computational time required to yield that relatives error. Starting in the top left of the graphs the smallest computation times and largest relative error occurs at the lartest value of $\Delta\tau$ while the longest run time and smallest error shown in the bottom right is a result of the largest $\Delta\tau$. There is an improvement of accuracy in all

Table IV. CF L1 Norm From Reference Solution for Each Spatial Width

$\Delta\tau\backslash\Delta x$	0.025	0.05	0.1
0.01	0.00081	0.00094	0.00082
0.02	0.00205	0.00218	0.00194
0.04	0.00377	0.00422	0.00386
0.05	0.00460	0.00530	0.00489
0.08	0.00707	0.00796	0.00738
0.1	0.01026	0.00937	0.00905

Table V. CF with Predictor-Corrector L1 Norm From Reference Solution for Each Spatial Width

$\Delta\tau\backslash\Delta x$	0.025	0.05	0.1
0.01	0.00039	0.00058	0.00053
0.02	0.00107	0.00127	0.00144
0.04	0.00227	0.00276	0.00296
0.05	0.00280	0.00366	0.00366
0.08	0.00437	0.00507	0.00583
0.1	0.00556	0.00651	0.00692

methods by simply decreasing the size of the time step, however, it should be noted that for equivalent values of $\Delta\tau$ and Δx the CF method is more accurate than the IMC method, and predictor corrector methods are more accurate than their cooresponding standard method.

6. Conclusions

The IMC method has a bias in the numerical solution of temperature that depends on the value of α. In the case of warming problems, the temperature of the material in the IMC calculation is lower than the correct solution. When using large time steps for a given opacity, this bias in effect helps the IMC solution yield more accurate results since too much energy should have been absorbed during that time step, leading to the offsetting of errors, as shown in the 0D solutions. However, in the 1D solutions the decreased material temperature affects the wave speed due to larger opacity estimates. These larger opacities slow the progress of the Marshak wave as compared to a comparable CF method or the refined reference solution. The effect of the bias in

Table VI. CF with 100 Variable Weight Predictor-Corrector L1 Norm From Reference Solution for Each Spatial Width

$\Delta\tau\backslash\Delta x$	0.025	0.05	0.1
0.01	0.00048	0.00060	0.00056
0.02	0.00097	0.00122	0.00148
0.04	0.00213	0.00307	0.00279
0.05	0.00282	0.00343	0.00353
0.08	0.00440	0.00515	0.00581
0.1	0.00581	0.00622	0.00689

the IMC method is minimized by decreasing the time step size.

The CF method has proven point for point to be more accurate than the IMC method in the 1D case, at the cost of more computational time. Likewise, the predictor-corrector methods are also an improvement on both IMC or CF at another computational expense. Determining whether the CF or predictor-corrector methods will be an overall computation-time per accuracy gain is a difficult task that may be code dependent. The timing results in this paper were conducted on a research code that lacks much of the complexity or tallies that will occur in a production level code.

ACKNOWLEDGEMENTS

This work was supported in part by the DOE NNSA under the Predictive Science Academic Alliances Program by grant DE-FC52-08NA28616

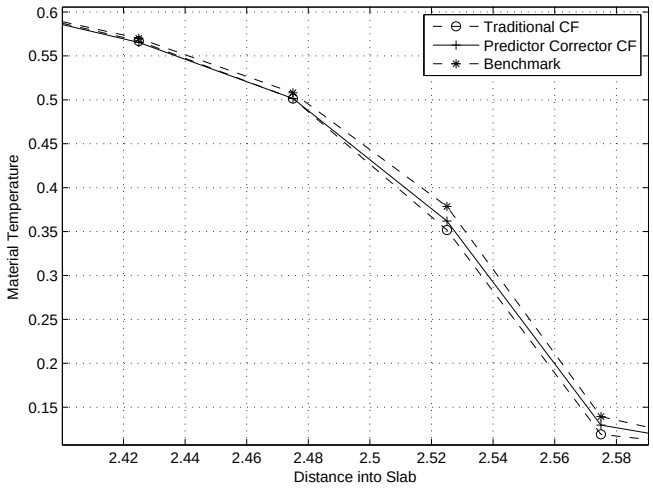

Figure 3. Marshak Wave front using CF at $\tau = 20$ with $\Delta\tau = 0.05$ and $\Delta x = 0.05$

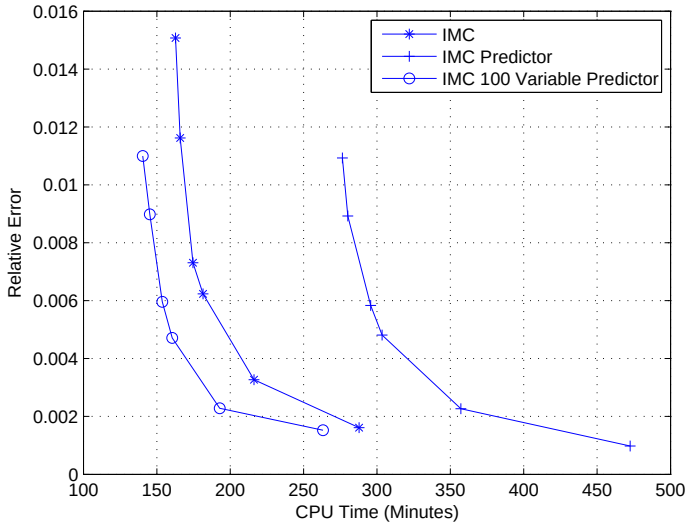

Figure 4. Relative Error of the IMC method vs. Time

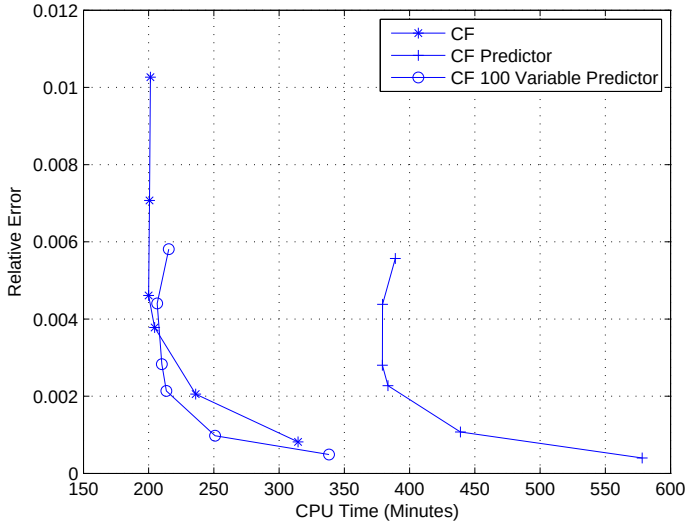

Figure 5. Relative Error of the CF method vs. Time

REFERENCES

1. J. A. Fleck and J. D. Cummings. An implicit monte carlo scheme for calculating time and frequency dependent nonlinear radiation transport. *Journal of Computational Physics*, 8:313, 1971.

2. Carter L.L. and Forest C.A. Nonlinear radiation transport simulation with an implicit monte carlo method. *LA-5038, Los Alamos National Laboratory*, 1973.

3. William R. Martin and Forrest B. Brown. Error modes in implicit monte carlo. *LA-UR-01-3755, Los Alamos National Laboratory*, 2001.

4. Scott W. Mosher and Jeffery D. Densmore. Stability and monotonicity conditions for linear, grey, 0-d implicit monte carlo calculations. *Transactions of the American Nuclear Society*, 93:520–522, 2005.

5. Scott W. Mosher. Exact solution of a nonlinear, time-dependent, infinite-medium, grey radiative transfer problem. *Transactions of the American Nuclear Society*, 95:744, 2006.

6. Allan B. Wollaber. *Advanced Monte Carlo Methods for Thermal Radiation Transport*. PhD thesis, University of Michigan, 2008.

7. William R. Martin and Forrest B. Brown. Comparison of monte carlo methods for nonlinear radiation transport. In *American Nuclear Society Math and Computation Slide Presentations*, 2001.